On the Feasibility of a Secondary Service Transmission over an Existent Satellite Infrastructure

Luciano Barros Cardoso da Silva[1(✉)], Tarik Benaddi[2], and Laurent Franck[3]

[1] IMT Atlantique, LabSTICC, Toulouse, France
luciano.barroscardosodasilva@imt-atlantique.fr
[2] IMT Atlantique, LabSTICC, DEOS, Toulouse, France
tarik.benaddi@imt-atlantique.fr
[3] Airbus Defence and Space, Toulouse, France
laurent.franck@airbus.com

Abstract. In this paper, we present a realistic use case in order to investigate the feasibility of a secondary service transmission over an existent satellite infrastructure. By introducing the overlay cognitive radio paradigm towards satellite communications, we compute a theoretical achievable data rate greater than 16 kbps for the secondary service, which is suitable for most M2M applications. Using simulation results, we show that this can be achieved while preserving the primary service performance. In addition, a system design framework is discussed in order to dimension such systems.

Keywords: Satellite communications · Cognitive radio · Overlay paradigm · Dirty paper coding · Machine-to-Machine application

1 Introduction

Machine-to-Machine (M2M) communications are one of the central use cases in the upcoming new fifth generation (5G) mobile network [1] as they play a major role in the internet of things (IoT). [2] predicts the deployment of around 1 million devices per km^2 like sensors/actuators, vehicles, factory machines, beacons *etc.* In this new machine-type communication environment and since available radio spectrum is today a scarce resource (cf [3] for example), one of the main faced challenges concerns the design of efficient spectrum utilization and a better coordination between legacy and future services.

Within this context, despite of the continuous technological developments in terrestrial networks, the satellite communications systems are still relevant in the modern telecommunications world. This affirmation can be sustained especially today, since the demand for the rising new services has experienced a significant growth, supported by the unique characteristics such as multicast

A. Kliks et al. (Eds.): CrownCom 2019, LNICST 291, pp. 154–167, 2019.
https://doi.org/10.1007/978-3-030-25748-4_12

and broadcasting capabilities, mobility aspects, global reach, besides the ability to cover and connect green space and hostile environments [4]. In this sense, the use of satellite for M2M applications provides to the end-users connectivity anytime, anywhere, for any media and device.

As a counterpoint, to meet these increasingly challenging requirements while keeping the competitiveness facing the terrestrial technologies, the satellite segment needs to push the boundaries in the direction to more and more efficient technical solutions. In this sense, the search for power and bandwidth efficiency as well as the actual trend to low complexity systems are of the upmost importance. It is within this framework that the terrestrial cognitive radio techniques have also attracted the attention for satellite applications. Supported by the recent developments in the space qualified Software Defined Radios (SDR) [5], and also by the maturity of concepts such as flexible [6] and hosted payloads, these techniques have become feasible whereby some relevant research have been developed, resulting in a more smart spectrum management.

In a nutshell, the cognitive user (CU), unlicensed or less prioritized to operate in a specific spectrum band, senses the environment around it and adapts its transmission as a function of the interference, by adjusting the frequencies, waveforms and protocols in order to access the licensed primary user (PU) spectrum efficiently. Without going into further details, three paradigms classifies the CU operation [7]:

- *interweave*, where the CU transmits opportunistically into the spaces not currently used by the PU;
- *underlay*, where the CU adjusts its parameters according to the PU signal characteristics in order to transmits simultaneously while respecting an interference power threshold;
- *overlay*, where the CU has the noncausal knowledge about the PU signal and message and, by using judiciously chosen coding and signal processing techniques, is able to use simultaneously the PU channel (same frequency, time and polarization), without deteriorating this latter.

The first two schemes were well studied in [8,9]. In this paper, we investigate the third scheme.

The main reason to propose the overlay paradigm for satellite communications lies in the feasibility of transmitting both unlicensed and licensed services simultaneously towards its respective terminals. We emphasizes that, due the priority among users, the superposition coding strategies is required [10], unlike the technical solutions adopted for the broadcast channel. In practice, this method enables the addition of a secondary service above legacy infrastructure of the primary service, instead of using a dedicated satellite or constellation.

This paper presents a practical scenario for the techniques previously exposed in the recent publications [11,12], which concern the design of the overlay paradigm transmission towards satellite communication systems. By using the concepts and the framework well characterized by these references, this work extends the previous analysis focusing on the feasibility of a low data rate

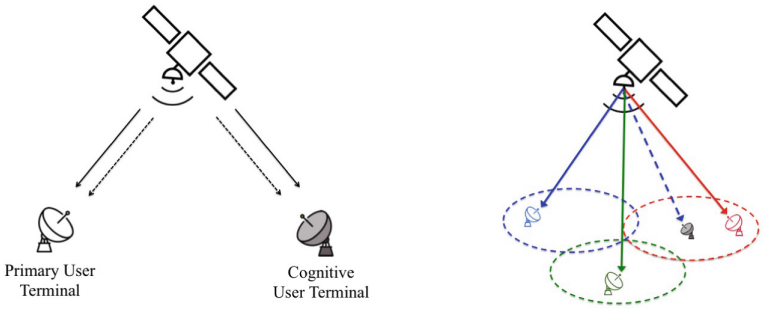

(a) LEO/MEO (b) GEO Multibeam

Fig. 1. Satellite scenarios (Color figure online)

transmission. In this sense, a practical use case is investigated, which considers commercial off-the-shelf (COTS) parts [13] and assumes realistic link budget parameters in its evaluation. The discussions and results contained herein could be seen as part of a "preliminary phase" of an engineering process plan [14].

2 Overlay Model Description

The following scenarios are provided as examples where the overlay CR techniques might be applied to satellite communications. In the first case, presented in the Fig. 1a, an ordinary LEO/MEO satellite provides two different services towards different terminals. In this context, a single licensed user PU takes priority over the added unlicensed CU. The interference presented at both terminals should be mitigated by properly designed CU encoder, without any changes in the PU transmission chain.

In the same way, the GEO multibeam satellite is illustrated in the Fig. 1b. In this case, considering the frequency reuse, the CU is able to transmits by using, for instance, the determined blue frequency (or polarization) into the red spot footprint, as far as the interference among adjacent beams is resolved. It is worth noting also that all possible different PU transmissions, represented by several blue spots, should be taken into account in the interference mitigation design. By this way, the total satellite capacity could be increased as well as the spectrum resources better managed.

Equally suitable for both scenarios, the interference model with side information, adapted from [10], is presented in Fig. 2. Assuming that the signals are onboard the satellite, the cognitive encoder has full and noncausal knowledge about each PU *i-th* signal and message, which addresses the main overlay paradigm requirement. In this sense, the encoded cognitive signal X_c^n is function of both primary and cognitive messages $m_{p,i}$ and m_c.

Without loss of generality, considering the *i-th* PU and the added CU, the channel gains $|h_{yx,i}|$ (from the transmitter x to the receiver y) are defined by

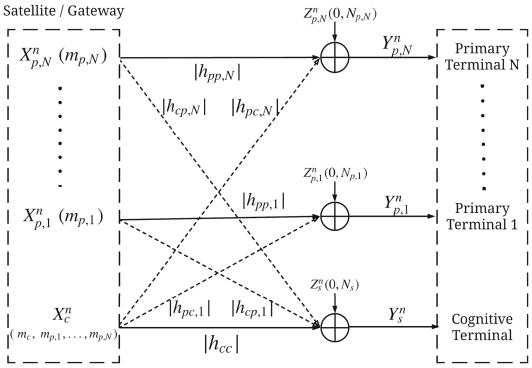

Fig. 2. Overlay model.

the direct paths ($|h_{cc}|$ and $|h_{pp,i}|$), and the interfering paths ($|h_{pc,i}|$ and $|h_{cp,i}|$) losses (the Fig. 2 summarizes these notation). In our context, these gains are computed as function of the each transmission link budget.

The following equations describes the output of the channel, where n refers to the *n-th* symbol:

$$Y^n_{p,i} = |h_{pp,i}|X^n_{p,i} + |h_{pc,i}|X^n_c + Z^n_{p,i} \tag{1}$$

$$Y^n_s = |h_{cc}|X^n_c + \sum_{i=1}^{N} |h_{cp,i}|X^n_{p,i} + Z^n_s, \tag{2}$$

Based on the fact that the terminals may be located in different geographical sites, the Gaussian noise component $Z^n_{p,i}$ (resp. Z^n_s) is assumed to follow the normal law $\mathcal{N}(0, N_{p,i})$ (resp. $\mathcal{N}(0, N_s)$). Also, the power constraints to be satisfied are $E[\|X^n_{p,i}\|^2] = P_{p,i}$ and $E[\|X^n_c\|^2] \leq P_c$, respectively.

Finally, since each PU has the same transmission priority, we highlight that the interference among them could be solved by precoding techniques as proposed, for instance, in DVB-S2X standard [15]. Under this assumption, this work provides a design method to permit a secondary service transmission without affecting the PU transmission performance.

3 Enabling Techniques

3.1 Superposition Strategy

The purpose of the superposition technique is to ensure that the signal-to-noise ratio (SNR) at each PU receiver is not decreased in the presence of interference. To accomplish this goal, the CU shares part of its power to relay each PU. Based on that operation, the CU transmitted signal is given by:

$$X^n_c = \hat{X}^n_c + \sum_{i=1}^{N} \sqrt{\alpha_i \frac{P_c}{P_{p,i}}} X^n_{p,i}, \tag{3}$$

where $\alpha_i \in [0,1]$ is the shared power fraction from P_c to relay each PU message.

Under the assumption that all signals are statistically independent, the new power constraint can be defined as $E[\|\hat{X}_c^n\|^2] \leq (1 - \sum_{i=1}^{N} \alpha_i)P_c$. The signal-to-interference-plus-noise ratio (SINR) at the *i-th* primary receiver is given by:

$$SINR_{P,i} = \frac{E\left[\|(|h_{pp,i}| + |h_{pc,i}|\sqrt{\alpha_i \frac{P_c}{P_{p,i}}})X_{p,i}^n\|^2\right]}{E[\||h_{pc,i}|\hat{X}_c^n\|^2] + E[\|Z_{p,i}^n\|^2]} = \frac{\|h_{pp,i}\|^2 P_{p,i}}{N_{p,i}} \tag{4}$$

In this context, the superposition factor $\alpha_i \in [0,1]$ that guarantees Eq. (4), for the interference condition ($|h_{pc,i}| > 0$), which is a generalized form of [10, Eq. 14], is given by:

$$\alpha_i = \left(\frac{|h_{pp,i}|\sqrt{P_{p,i}}\left(\sqrt{N_{p,i}^2 + \|h_{pc,i}\|^2 P_c(N_{p,i} + \|h_{pp,i}\|^2 P_{p,i})} - N_{p,i}\right)}{|h_{pc,i}|\sqrt{P_c}(N_{p,i} + \|h_{pp,i}\|^2 P_{p,i})} \right)^2 \tag{5}$$

By inspection of Eq. (3), we emphasize that the CU transmission is feasible only if the condition $\sum_{i=1}^{N} \alpha_i < 1$ is satisfied. By this assumption, note that the CU data rate should be decreased when aggressive frequency reuse scenarios are considered.

3.2 Dirty Paper Coding

Once the superposition factors are computed and the CU partially shares its power to relay each PU signal, the next step is to design $\hat{X}_c^n$ efficiently, in order to minimize the PU interference. The optimal strategy uses the theoretical results presented by Costa [16]. On the assumption that the interference is non-causally known at transmitter, a transmitter-based interference presubtraction can be implemented, without any power increase, reaching the AWGN capacity. In this sense, according to the main concept of this technique, the CU adapts its waveform, instead of cancel, as a function of the channel interference.

By rearranging the Eq. (2) and considering the superposition, we have:

$$Y_s^n = |h_{cc}|\hat{X}_c^n + \sum_{i=1}^{N} \left(|h_{cp,i}| + |h_{cc}|\sqrt{\alpha_i \frac{P_c}{P_{p,i}}} \right) X_{p,i}^n + Z_s^n. \tag{6}$$

Without loss of generality, given that the signals in Eq. (6) are statistically independents each other, the implemented model considers a single Gaussian distributed PU constellation, in respect to the total interfering power received at CU terminal. In addition, in order to simplify the notation through this paper, the Eq. (6) is normalized by the direct path attenuation factor $|h_{cc}|$. Thus, the signal at CU receiver is given by:

$$Y_s^n = \hat{X}_c^n + \underbrace{\left(b + \sqrt{\alpha \frac{P_c}{P_p}} \right) X_p^n}_{S^n} + Z_s^n, \tag{7}$$

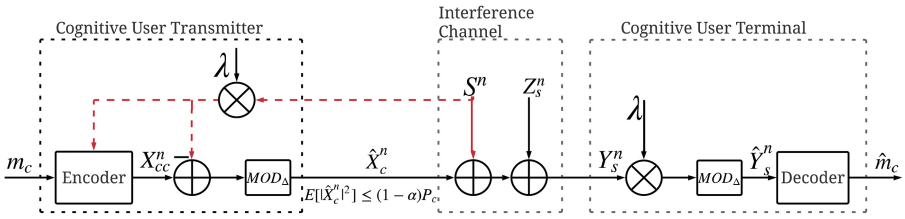

Fig. 3. Proposed DPC encoder.

where the factor b represents the normalized interfering path and S^n represents the total channel interference.

The Fig. 3 presents the basic diagram of the DPC encoder. In this configuration, assuming low and intermediate SNR regime, the partial interference presubtraction (PIP) is implemented [16]. In this way, the signal $\hat{X}_c^n$ is designed as:

$$\hat{X}_c^n = \left[X_{cc}^n - \lambda S^n\right] \text{MOD}_\Delta, \tag{8}$$

where X_{cc}^n is the coded signal and the factor λ, to be properly chosen, controls the fractioned interference to be presubtracted. Also, MOD_Δ is the complex-valued modulo operation. The modulo amplitude is defined by $\Delta = \sqrt{M} d_{min}$, where M is the number of points of the square QAM constellation and d_{min} the minimum intersymbol distance.

Concerning the historical perspective for practical DPC implementations, the use of Tomlinson-Harashima precoding (THP) for intersymbol interference (ISI) cancelling was firstly introduced by Erez et al. in [17]. Subsequently, Eyuboglu and Forney [18] developed the trellis precoding technique (TP), also recovering partially the so-called shaping loss by the trellis shaping (TS) technique [19]. Finally, the TP technique for multiuser interference, presented in [20] further developed in [21], formed the basis of our implemented DPC encoder.

The Fig. 4 details the practical DPC encoder implemented in this work. Three separated gains can be reached by this system:

- the coding gain, which is realized by the coset select code C_c, specified G_c;
- the shaping gain, generated by the shaping code C_s, according to the TS technique [19] for multiuser interference;
- the precoding gain, which mitigates the interference by the presubctraction combined with the shaping metric and modulo operation.

This work implements the following branch metric Eq. (9), where the precoder selects the proper region sequence with minimum average energy to steer the scaled interference sequence λS, taking also account the modulo operation.

$$\| \left[X_{cc}^n - \lambda S^n\right] \text{MOD}_\Delta \|^2. \tag{9}$$

The Fig. 5 presents the scatter plot of the signals corresponding to the encoder processing. The 16-QAM and further 256-QAM expanded constellations signal

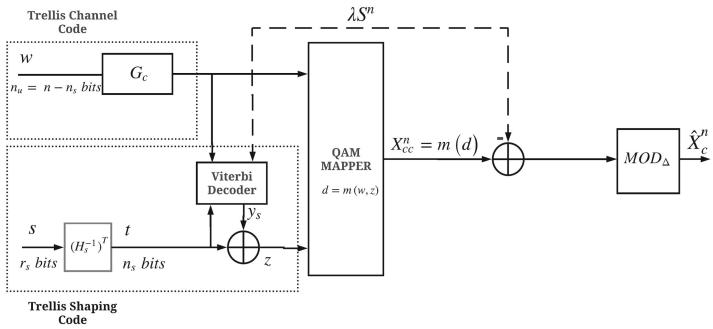

Fig. 4. Proposed DPC encoder [12]

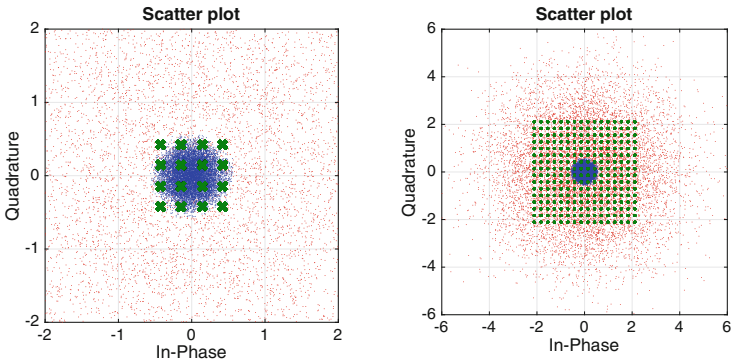

(a) DPC 16-QAM (b) DPC 256-QAM

Fig. 5. Scatter Plot of Signal Constellation at CU Transmitter, considering $10.log(Pp/Pc) = 9.5$ dB and $\alpha = 0.85$, according with the use case of this paper (X_{cc}^n in green "x", λS^n in red dots and $\hat{X}_c^n$ in blue dots). (Color figure online)

X_{cc}^n is shown superposed by the gaussian distributed scaled interference λS^n, considering the study case presented in the next section. The transmitted signal $\hat{X}_c^n$, after presubtraction and modulo operation, is also illustrated by the blue dots. We highlight that, despite of the large amount of interference, the transmitted signal is confined into the expanded constellation, respecting the power constraint of the DPC theory. In addition, we can note that further expansion can be done to confine the total interference [12]. However, the complexity of the system will be increased.

At the receiver, the reverse operations are done. In this sense, at the decoder input, the signal is given by:

$$\hat{Y}_s^n = \Big[(\hat{X}_c^n + S^n + Z^n)\lambda\Big] \text{MOD}_\Delta. \tag{10}$$

Finally, the choice of the λ is done with the goal to maximize the equivalent CU signal to noise ratio (SNR) in Eq. (10). The λ factor can be optimized and is given by [16]:

$$\lambda = \frac{(1-\alpha)P_c}{(1-\alpha)P_c + E[|Z_s^n|^2]}. \tag{11}$$

3.3 CU Transmitted Power

By reason of the TP operation, a power reduction of $\hat{X}_c^n$ is obtained, which impacts directly both links performance as follows:

- For the PU, by inspection of Eq. (4), it is noticed that this power reduction will result in an increase of the SINR at the PU receiver (in comparison to the case with no interference). This occurs because the superposition factor α in Eq. (5) does not take into account the shaping gain induced by TP. Consequently, the PU link would present a better BER performance than that required;
- Concerning the CU, it is also noted that under these conditions, we obtain $E[|X_c^n|^2] < P_c$. This means that the CU is not operating in its total power capacity. Consequently, this will lead to an under utilization of the available resources on the satellite.

The proposed method for controlling the CU output power, presented in [12], allows to reach the power equality $E[|X_c^n|^2] = P_c$ (or equivalently, $E[|\hat{X}_c^n|^2] = (1-\alpha)P_c$) as a function of the shaping gain. This is obtained by an adequate scaling of the minimum distance d_{min} of the cognitive transmitted constellation. In short, according to this method, we define the power of the baseline, without considering the shaping operation (i.e. uniformly distributed constellation points), as:

$$P_{\oplus} = \frac{2^R}{6} d_{min}{}', \tag{12}$$

where R is the data rate in bits per two dimensions. In addition, the shaping gain is given as follows:

$$\gamma_s = \frac{P_{\oplus}}{(1-\alpha)P_c}. \tag{13}$$

As a consequence, we define the scaled minimum distance $d_{min}{}'$, such that the available power after the shaping operation is equals to $(1-\alpha)P_c$, as:

$$d_{min}{}' = \sqrt{\frac{[(1-\alpha)P_c]6\gamma_s}{2^R}}. \tag{14}$$

Based on this proposed design procedure exposed in this section, the trellis-shaped based DPC encoder using a M-QAM expanded constellation at the transmission rate of $R_{cu} = 2$ bits/symbol was implemented for the proposed use case of the next section. Further analyses and the complete characterization of the performance as well as the distortions evolved can be find in [12]. In the next section, we investigate the feasibility in a realistic application.

3.4 Practical System Analysis

As a matter of system engineering, the design for the CU payload could either be a standalone system (implemented by a dedicated transmission chain and antenna) or a shared transmitter (by using the same transponder and antenna as the PU). In this latter configuration, notice that more caution should be taken into account when the transmission of both signals inputs the same high power amplifier (HPA). In fact, this practice should be avoided since this implementation may induce higher nonlinear distortions, particularly in terms of AM/AM and AM/PM conversions [22].

Moreover, at the receiver side (PU and CU), two design solutions could be adopted: (i) by the deployment of geographically separated receiving sites for each user, in this way reducing the interference due to the attenuation at the interfering paths, or (ii) by using the same receiving station with two dedicated demodulators and decoders. In this last case, the attenuation of the interfering and direct paths are the same (i.e. $|h| = |h_{pp,i}| = |h_{cc}| = |h_{pc,i}| = |h_{cp,i}|$). In fact, it increases the interference of both links and, as a consequence, requires higher value of the superposition factor α (in other words, reducing the secondary service data rate). On the other hand, we reduce the infrastructure costs, since the hardware is further simplified by utilizing the same earth station to receive also the CU signal.

Deepening the vision on the techniques described, we point out that, due to the superposition, the bit rate of the secondary service might be very low with respect to the primary. However, this practice generates two implementation problems: (i) in the DPC presubtraction technique, the same symbol rate for both signals is considered in order to be able to compute the Eq. (8) and (ii) in the superposition technique, the interference generated by the CU signal would appears as spikes in the PU bandwidth, which makes the usual interference model unrealistic in this case. In order to avoid both constraints, we can think of the implementation of the chirp spread spectrum technique [23] at CU transmission. In this sense, the DPC encoder can correctly perform its operation and the CU receiver can demodulated at a more flexible transmitted data rate.

To improve the whole system performance, the channel estimation techniques could be realized at the terminals end through a link feedback, for instance, according to the DVB-S2X standard [15]. By these features, the superposition factor α, which depends directly on the channels conditions, as well as the λ, which depends on SNR, can be periodically updated, changing the achievable secondary service data rate and, as consequence, optimizing CU performance.

4 Realistic Use Case

In order to investigate the system feasibility, we adopted a scenario where a Cubesat at a height of 600 km with same orbital parameters as [24], using COTS parts, transmits both signals (primary and cognitive) from the same satellite antenna towards a single earth station, which is equipped with two dedicated

demodulators. In this sense, the channel attenuations are the same and defined as $|h|$. In this study, just the downlink is considered.

The main specification for the PU signal are: output power of $1W$ [13], operating frequency of 2200 MHz (downlink band assigned for Earth Exploration Satellite Service), bit rate of 3.4 Mbps, BER specified to 10^{-5} and coded QPSK modulation with FEC ($R = 1/2$). The following Table 1 presents the link budget of PU without secondary service addition.

Table 1. Primary user link budget (QPSK Coded FEC R = 1/2).

Frequency (MHz)	2200
Throughput rate (Mbps)	3.4
Transmitted power (mW)	1000
Satellite carrier EIRP (dBm)	38.3
Free space loss (dB)	−162.2
Depointing loss (dB)	−10
E. S. Antenna max gain - 5 m, eff 50 % (dBi)	38.2
System noise temperature (K)	130
C/N0 (dB-Hz)	81.8
Eb/N0 (dB)	16.5
Demodulation losses (dB)	−6
Eb/N0 required (dB) – for BER = 1E-5	7
Margin (dB)	3.5

It is worth noting that a conservative margin for demodulation losses of 6 dB is assumed in order to cover the impairments of the communication chain. The overall link margin is about 3.5 dB, as required by the targeted BER.

The principle behind this design strategy was to use part of the power remaining in this margin to transmit the CU signal. Therefore, we defined that 900 mW were allocated for PU transmission (which still maintain the recommended link margin of 3 dB) and 100 mW were used for CU. The next Fig. 6 presents the overlay model considering this use case.

The powers transmitted and received are provided considering the realistic link budget parameters. By computations according the Table 1, the channel attenuations equal $\|h\|^2_{dB} = -125.7$ dB. In this condition, the interference-to-noise ratio (INR) and the link degradation D by interference are given by:

$$INR = \frac{I_{pc}}{N_p} = 4.47; \tag{15}$$

$$D(dB) = 10.log(1 + INR) = 7.38\ dB. \tag{16}$$

The CR overlay techniques are employed to mitigate both link degradation. Firstly, considering all parameters, the CU performs the superposition strategy

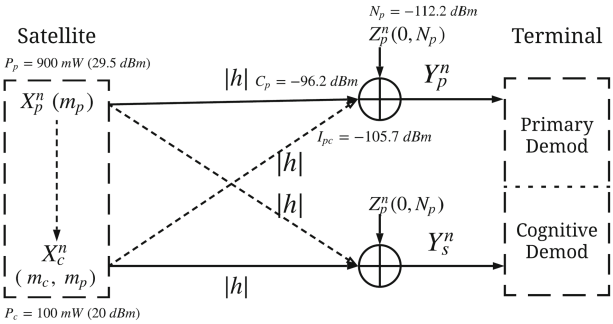

Fig. 6. Overlay model considering realistic satellite link budget.

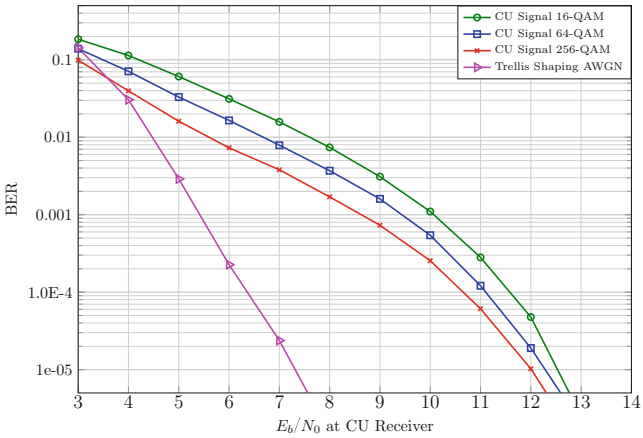

Fig. 7. BER CU, considering $10.log(Pp/Pc) = 9.5$ dB and $\alpha = 0.85$, according with the use case.

and, by the Eq. (5), the factor $\alpha = 0.85$ is evaluated. This value guarantees a $SINR$ of 16 dB at PU. We highlight that, thanks to the superposition strategy and the power controlling design of the DPC encoder (see results in [12]), the PU maintains the same performance as in absence of the CU interference.

From this point, a simulation for CU link is realized considering the whole CU channel interference (see Eq. (7)), which is composed by the PU signal and the CU shared power in the superposition.

By taking the link parameters and the CU BER curve presented in Fig. 7, we can now compute the link budget, presented at Table 2. It is important to note that, by reason of superposition, just 15 % of the power originally allocated for CU is used for its own transmission. However, despite of the low power received, the sensitivity of the receiver is in line with the specifications usually attributed for small satellites links (i.e. sensitivity threshold of −118 dBm [25]).

We emphasize that all conservative margins are still being considered in order to guarantee the performance.

Table 2. Cognitive user link budget.

Transmitted power (mW)	100 * 0.15
Satellite carrier EIRP (dBm)	20.1
Free space loss (dB)	−162.2
Depointing loss (dB)	−10
Ground station antenna max gain - 5 m, eff 50 % (dBi)	38.2
System noise temperature (K)	130
C (dBm)	−113.9
C/N0 (dB-Hz)	63.6
Demodulation losses (dB)	−6
Eb/N0 required (dB) – for BER = 1E-3	
DPC 16-QAM	10
DPC 64-QAM	9.4
DPC 256-QAM	8.5
Eb/N0 required (dB) – for BER = 1E-5	
DPC 16-QAM	12.5
DPC 64-QAM	12.25
DPC 256-QAM	12
Margin (dB)	3
Minimum Bit Rate (kbps) – DPC 16-QAM	
BER = 1E-3	28.8
BER = 1E-5	16.2
PAPR	
DPC 16-QAM	5.0
DPC 64-QAM	4.67
DPC 256-QAM	4.79

It is worth noting that different M-QAM schemes present the peak to average power ratio (PAPR) in the same order of magnitude. Also, the further expansion impacts directly in the BER performance, even when the total interference is not confined inside the expanded constellation (as in this case). As pointed in [11], by practical effects, the SNR here does not consider the defined effective noise in Eq. (11). It could suggest that DPC performs better than AWGN in low SNR, which is not the case. As an important result of this feasibility analysis, we assure that the bit rate of 16 and 28 kbps can be reached for the secondary service, as a function of the BER specified, which depends on the service application.

5 Conclusion

This paper investigated the feasibility of a low data rate secondary service transmission over a primary user infrastructure. A realistic scenario was presented with COTS parts and the different techniques were implemented to resolve the interference of both links. As a result, we obtained the same performance for the PU as in absence of the CU operation (AWGN channel). Concerning the secondary service, we have reached a data rate greater than 16 kbps, which is suitable for most of M2M applications.

As a drawback, we point out an increase of the output power of the satellite due to the intrinsic signal correlation presented at the superposition technique. In the described scenario, the total power transmitted is about 32 dBm instead of 30 dBm specified. In this case, the transmitted antenna should be properly designed in order to consider this output power.

Considering future works, we will seek another proof of concept by means of SDR implementation. In addition, the control of PAPR by shaping operation, typically on satellite communication, will be also investigated.

Acknowledgment. This work was supported by National Council for Scientific and Technological Development (CNPq/Brazil) and by National Institute for Space Research (INPE/Brazil).

References

1. ITU-R: Emerging trends in 5G/IMT2020. Geneva Mission Briefing Series, September 2016
2. Huawei: 5G network architechture - a high-level perspective. White paper, December 2016
3. United States radio spectrum frequency allocations chart. United States Department of Commerce (2016). https://www.ntia.doc.gov/files/ntia/publications/january-2016-spectrum-wall-chart.pdf
4. Minoli, D.: Innovations in Satellite Communications and Satellite Technology: The Industry Implications of DVB-S2X, High Throughput Satellites, Ultra HD, M2M, and IP. Wiley, Hoboken (2015)
5. Maheshwarappa, M.R., Bowyer, M., Bridges, C.P.: Software defined radio (SDR) architecture to support multi-satellite communications. In: IEEE Aerospace Conference, pp. 1–10 (2015)
6. Porecki, N., Thomas, G., Warburton, A., Wheatley, N., Metzger, N.: Flexible payload technologies for optimising Ka-band payloads to meet future business needs. In: Proceedings of the 19th Ka Broadband Communications, Navigation and Earth Observation Conference, pp. 1–7 (2013)
7. Biglieri, E.: An overview of cognitive radio for satellite communications. In: IEEE First AESS European Conference on Satellite Telecommunications (ESTEL), pp. 1–3 (2012)
8. Sharma, S.K., Chatzinotas, S., Ottersten, B.: Cognitive radio techniques for satellite communication systems. In: IEEE 78th Vehicular Technology Conference (VTC Fall), pp. 1–5 (2013)

9. Álvarez-Díaz, M., Neri, M., Mosquera, C., Corazza, G.: Trellis shaping techniques for satellite telecommunication systems. In: IEEE International Workshop on Satellite and Space Communications, pp. 148–152 (2006)
10. Jovicic, A., Viswanath, P.: Cognitive radio: an information-theoretic perspective. IEEE Trans. Inf. Theory **55**(9), 3945–3958 (2009)
11. da Silva, L.B.C., Benaddi, T., Franck, L.: Cognitive radio overlay paradigm towards satellite communications. In: 2018 IEEE International Black Sea Conference on Communications and Networking (BlackSeaCom), pp. 1–5 (2018)
12. da Silva, L.B.C., Benaddi, T., Franck, L.: A design method of cognitive overlay links for satellite communications. In: IEEE 9th Advanced Satellite Multimedia Systems Conference and the 15th Signal Processing for Space Communications Workshop (ASMS/SPSC), pp. 1–6 (2018)
13. ISIS high data rate S-band transmitter mission specifications (online). https://www.isispace.nl/wp-content/uploads/2016/02/isis-communication-systems-brochure-v2-compressed.pdf
14. DVB: DVB-doc A-172 white paper on the use of DVB-S2X for DTH applications DSNG and professional services broadband interactive services and VL-SNR applications (2015)
15. E.-M. ECSS: ST-10C: Space project management-project planning and implementation (2009)
16. Costa, M.: Writing on dirty paper (corresp.). IEEE Trans. Inf. Theory **29**(3), 439–441 (1983)
17. Erez, U., Shamai, S., Zamir, R.: Capacity and lattice strategies for canceling known interference. IEEE Trans. Inf. Theory **51**(11), 3820–3833 (2005)
18. Eyuboglu, M.V., Forney, G.D.: Trellis precoding: combined coding, precoding and shaping for intersymbol interference channels. IEEE Trans. Inf. Theory **38**(2), 301–314 (1992)
19. Forney, G.: Trellis shaping. IEEE Trans. Inf. Theory **38**(2), 281–300 (1992)
20. Yu, W., Varodayan, D.P., Cioffi, J.M.: Trellis and convolutional precoding for transmitter-based interference presubtraction. IEEE Trans. Commun. **53**(7), 1220–1230 (2005)
21. Sun, Y., Xu, W., Lin, J.: Trellis shaping based dirty paper coding scheme for the overlay cognitive radio channel. In: IEEE 25th Annual International Symposium on Personal, Indoor, and Mobile Radio Communication (PIMRC), pp. 1773–1777 (2014)
22. Maral, G., Bousquet, M.: Satellite Communications Systems: Systems, Techniques and Technology. Wiley, Hoboken (2011)
23. Proakis, J.G., Salehi, M.: Digital Communications, vol. 4. McGraw-Hill, New York (2001)
24. Barbarić, D., Vuković, J., Babic, D.: Link budget analysis for a proposed cubesat earth observation mission. In: 2018 41st International Convention on Information and Communication Technology, Electronics and Microelectronics (MIPRO), pp. 0133–0138. IEEE (2018)
25. Arias, M., Aguado, F.: Small satellite link budget calculation. In: ITU Symposium and Workshop on Small Satellite Regulation and Communication Systems (2016)